

Development of a Nonhydrostatic Icosahedral High-resolution Atmospheric General Circulation Model

Group Representative

Masaki Satoh Integrated Modeling Research Program, Frontier Research System for Global Change, Sub-Group leader

Authors

Masaki Satoh Integrated Modeling Research Program, Frontier Research System for Global Change, Sub-Group leader

Hirofumi Tomita Integrated Modeling Research Program, Frontier Research System for Global Change, Researcher

Koji Goto HPC Marketing Promotion Division, Scientific Software Department, NEC Corporation

Tomoe Nasuno Integrated Modeling Research Program, Frontier Research System for Global Change, Researcher

A new atmospheric general circulation model is being developed at Frontier Research System for Global Change. It is a gridpoint model with an icosahedral grid and is based on the nonhydrostatic equations. The main target is high-resolution climate simulation by improving representation of cumulus convection with much higher resolutions. Since this project started at the year 2000, continuous effort has been made to develop the new global model. We have just completed the development of its dynamical core. For investigation of physical processes in super high-resolutions, we have developed another nonhydrostatic model, which is a regional Cartesian model and scheme of which is essentially same as in the global model.

In this paper, we describe the strategy of model development, the model description, and several results on the Earth Simulator. We have also examined the computational performance of our global model on the Earth Simulator and compared with that of a well-tuned spectral transform model. As a result, we found that the gridpoint method using an icosahedral grid has computational advantage over the spectral transform method in the higher resolution than about T1000.

Keywords: icosahedral grid, global nonhydrostatic model

1. Overview

The aim of this project is to develop a next generation atmospheric general circulation model (AGCM) for climate studies. We intend to run this model with super high-resolutions such as 5km or less in the horizontal directions and 100m in the vertical. In such a high-resolution simulation, we can expect to capture more accurate structures of the global atmosphere without any cumulus parameterization, which is one of the most uncertain factors in the current climate models. For this purpose, we have been taking three paths of the development since the starting point of this project (the year 2000).

First, it has been necessary to choose the nonhydrostatic equations as the governing equations for the new model instead of the hydrostatic primitive equations since the starting point. Although there has been many established regional nonhydrostatic models that are proved to be successful in short range numerical simulations, these models are not suitable to long term integrations as climate simulation. This is mainly because conservations for several important quantities are not well considered in their numerical

schemes. Since our new nonhydrostatic model is aimed to be used for climate studies, we have engaged in development a new dynamical scheme that can run for long time duration with conserving mass and energy (Satoh, 2002a, 2003).

Second, we had to choose simultaneously a proper method for solution of horizontal dynamics at the high-resolution simulation. It has been pointed out that the computational performance of spectral transform models and the latitude-longitude gridpoint models will be severely limited as the resolution increases. We chose to employ a gridpoint method using a quasi-uniform grid system represented as an icosahedral grid and a cubic grid. Constructing global shallow water models based on these grid systems, we examined their computational accuracies and efficiencies. Through this preliminary investigation, we have decided to choose an icosahedral grid (Fig.1) as the grid system of our new AGCM (Tomita et al., 2001, 2002)

Third, we have studied physical processes suitable to the new global model. Typical AGCMs currently used have 100km-scale horizontal-resolution, and the physical processes such as cumulus convection, radiation, and turbulence in

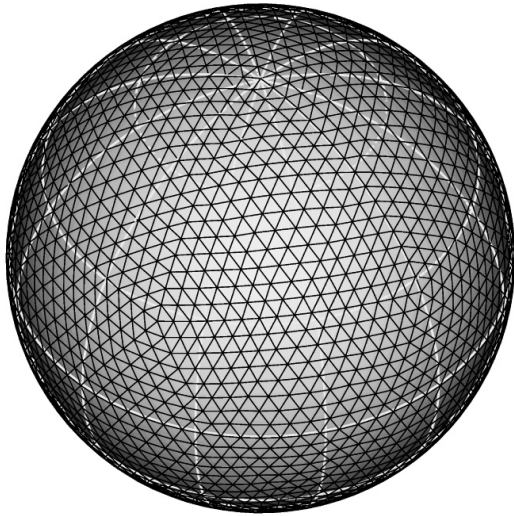


Fig. 1 The icosahedral grid structure (glevel-4). See text for mean of "glevel".

these models have been developed or tuned for this particular scale. Since our new high-resolution model is aimed to be run in 10km or less horizontal-resolution, it cannot be expected that the existing cumulus parameterizations based on statistical equilibrium work well. Although we believe that the best approach is to explicitly resolve cumulus convections without any parameterizations, it is not clear whether the model with the 10km grid interval will reproduce realistic cumulus properties. Nasuno and Saito (2002) is one of the investigations of physical processes to be encountered in our model development.

Our tentative goal is to integrate the above three paths and develop a global cumulus resolving model. At the beginning of the year 2003, we have almost finished the development of a dynamical core of the three-dimensional global model using the icosahedral grid and the newly developed nonhydrostatic scheme (Tomita et al., 2003). We call this model the Nonhydrostatic ICosahedral Atmospheric Model (NICAM). Since we are now making a new AGCM from scratch, we have to confirm that the new model does really produce comparable results to those of the existing established models in the currently used horizontal-resolution and also to show in what sense the new model produces better results than those of the existing models.

In Section 2, we describe outlines of the nonhydrostatic modeling and show numerical results of cumulus convection obtained by our regional model, which is constructed in the Cartesian coordinates as a subset of NICAM. In Section 3, we describe the dynamical framework of NICAM and the results obtained in FY2002 on the Earth Simulator (ES). In Section 4, we discuss the computational performance of NICAM and compare it with that of a spectral transform model. In Section 5, we give the concluding remarks and list up further tasks.

2. Nonhydrostatic modeling

Our nonhydrostatic scheme is based on Satoh (2002a). This numerical scheme is briefly summarized as follows. The flux form equations of the fully compressible system are used as the governing equations, i.e., without any modification of the Euler equations. The orographic effect is treated with the terrain following coordinate. A difference from other existing nonhydrostatic models is that the internal energy is used as a prognostic variable instead of the pressure.

The time-splitting method is used for the integration of fast modes such as sound waves and gravity waves. These are integrated with a small time step, while the remaining slow modes are updated with a large time step, where either the leapfrog scheme or the second order Runge-Kutta scheme can be chosen. At the small time step integration, we use the flux division method, in which only the deviations from the values at large step time are updated for the evaluation of the flux terms; the horizontal components of momentum are integrated explicitly and the other variables, i.e., the density, the vertical momentum, and the internal energy are integrated implicitly through solving a one-dimensional Helmholtz equation for the vertical momentum; after solving for the vertical momentum, the density is integrated in the flux form; then we adopt an energy correction by using the flux form equation of the total energy instead of the internal energy equation to ensure the conservation of the total energy. This procedure guarantees the conservation of the density, the momentum, and the total energy. We can easily introduce a hydrostatic/nonhydrostatic option to the vertical momentum equation.

For the expressions of moist variables, more accurate formulas than the customary ones are used by taking account of the temperature dependency of latent heat and the effects of heat contents of water substance with all the specific heats being constant (Satoh, 2003). We follow the formulation of precipitation given by Ooyama (2001). In the flux form equations, transports of momentum and energy in addition to water mass are taken into account, and the energy transformation from the potential energy of rain to the internal energy are properly evaluated. These transports are calculated using an accurate one-dimensional conservative semi-Lagrangian scheme (Xiao et al., 2003).

Gross et al., (2002) pointed out that the advection of a tracer should be consistently constructed from the equation of density. In our scheme, the advection term of a tracer including water substance is calculated at large time steps, but the density is updated at every small time step. Although it seems to be inconsistent due to different integration time steps, we have developed a consistent method by using the average mass flux over the large time step for calculation of advection term of a tracer (Satoh, 2002b).

For validation of our nonhydrostatic scheme, we performed the squall line experiments proposed by

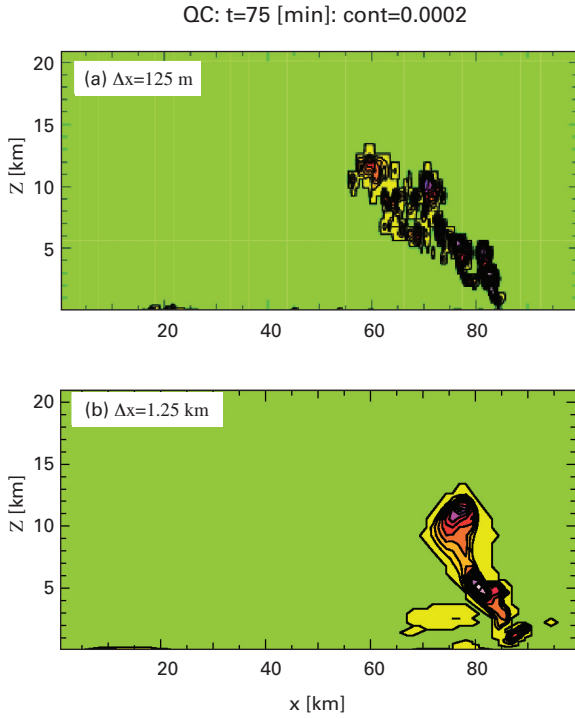


Fig. 2 Cloud water for the two-dimensional experiment of a squall line at time 75 min. Contour interval is 0.2 g kg^{-1} .

Redelsperger et al. (2002). The turbulence model, the surface process, and the radiation scheme that are used in CCSR/NIES AGCM 5.6 (Numaguti et al., 1995) have been installed. Only the warm rain process based on the bulk method is introduced and ice phase is not yet installed.

The first test case is a two-dimensional narrow region experiment with a horizontal domain size of 100km. In this test case, only one cloud is excited by an initial forcing and there occurs no successive cloud. However, this test case is suitable to investigation of parameter dependency in the

deterministic stage of a cloud evolution. We use the fourth-order numerical diffusion with the coefficient $\nu = \gamma \Delta x^4 / \Delta t \text{ m}^4 \text{ s}^{-1}$, where Δx , Δt , and γ denote the grid interval, the time interval in the large time step, and non-dimensional coefficient, respectively; we choose the decay time for the Δx -scale to be 10min. Figure 2 shows distributions of cloud water for the different grid intervals $\Delta x = 1.25 \text{ km}$ and 125 m . In both cases the evolutions of the cloud are similar, so that it suggests the validity of the coarser resolution simulation with $\Delta x = 1.25 \text{ km}$. We found that the evolution of cloud is very sensitive to numerical diffusion, i.e., its dependency on turbulence model is secondary.

The next case is a three-dimensional experiments of a squall line with a horizontal domain size of 100km times 125km and with a grid interval of 1.25km. Figure 3 shows potential temperature deviations from a reference profile at height 192m at time 150 and 200min. It can be seen that the cold pool is formed in arch shape, and is propagating with the squall line. It may be pointed out the following discrepancies with other model results; no clear anvil is developed aloft since only the warm process is used, and cloud activity is weakened at this time since the domain size is small. Nevertheless, the fact that many realistic properties can be reproduced encourages our new model development.

3. Nonhydrostatic Icosahedral Atmospheric Model

Using the almost same scheme as described in the previous section, we have developed a global dynamical core (Tomita et al., 2003) on the icosahedral grid depicted in Fig.1. Starting from the spherical icosahedron, the grid system is refined by the recursive way; one-level finer grids are generated by bisecting the geodesic arcs of the coarser grids. We call the grid system by n -th bisection glevel- n . The aver-

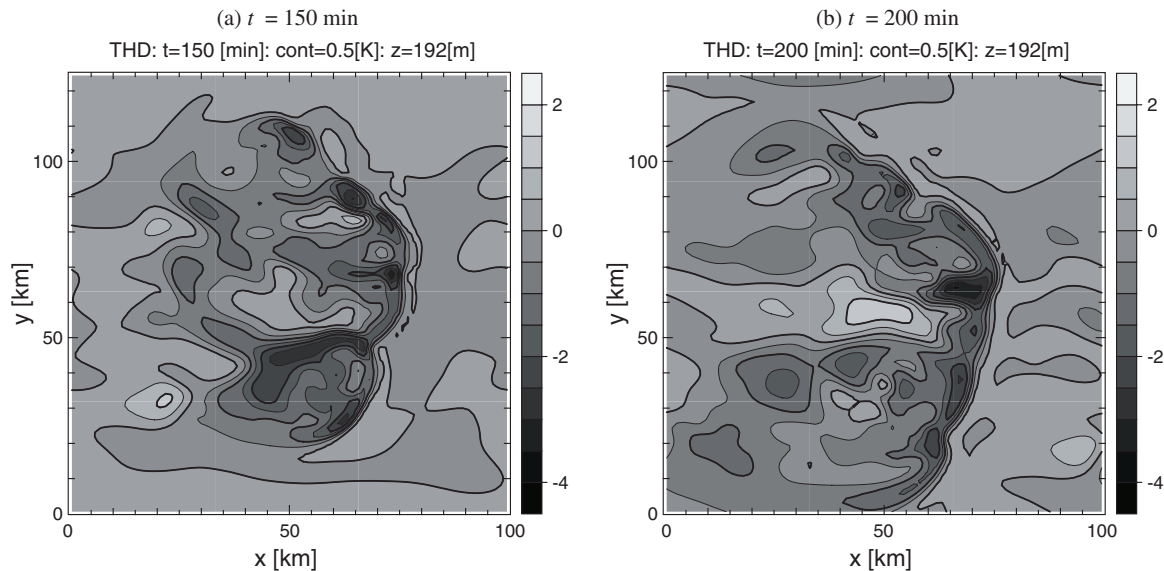


Fig. 3 Horizontal section of potential temperature deviations at the lowest level for the three dimensional squall line experiment (0.5 K interval).

age grid interval of glevel-10 is about 7.5km, for example. We modify thus generated icosahedral grid for the reduction of numerical errors; after the smoothing the grid arrangement by spring dynamics, the grid points are moved to gravitational centers of control volumes (Tomita et al., 2001, 2002). In addition, our icosahedral grid system has wide flexibility; it can be further modified to any structure as long as the geometric relations between the grid points are preserved. For instance, we can construct a stretched grid by concentrating grids at some locations in Asia with coarsening resolutions in the other hemisphere. This stretched grid model can be used as a regional climate model.

We show the results from the dynamical core of NICAM. The first test case is Held and Suarez (1994) Test Case

(HSTC). The results are compared with those of the spectral model called AFES¹ (AGCM for the Earth Simulator, Shingu et al. (2002); Ohfuchi et al., (2003)). We use the same fourth-order numerical diffusion in both of models ($\nu = 1.56 \times 10^{14} \text{ m}^2 \text{ s}^{-1}$). Figure 4 shows the meridional distribution of the zonal winds for averaging 1000days; the horizontal-resolutions are glevel-7 ($\Delta x \approx 60\text{km}$) for NICAM and T319 for AFES. The number of vertical layers is 30 for both models. The figure shows that the result of NICAM is almost comparable to that of AFES. We also found that the meridional structure of the eddy heat flux and the eddy momentum flux are almost the same between the two models. These

¹ AFES is a spectral transform model highly optimized on the ES and has full physical processes. We use the dynamical core of AFES for the HSTC experiment.

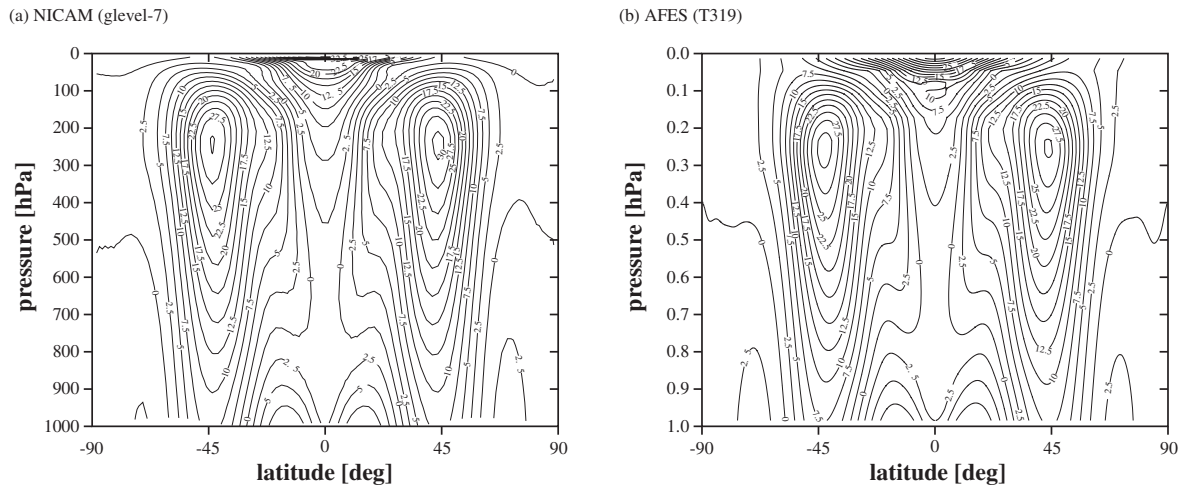


Fig. 4 Meridional distributions of zonal winds for HSTC averaged over 1000days (2.5 m s^{-1} interval).

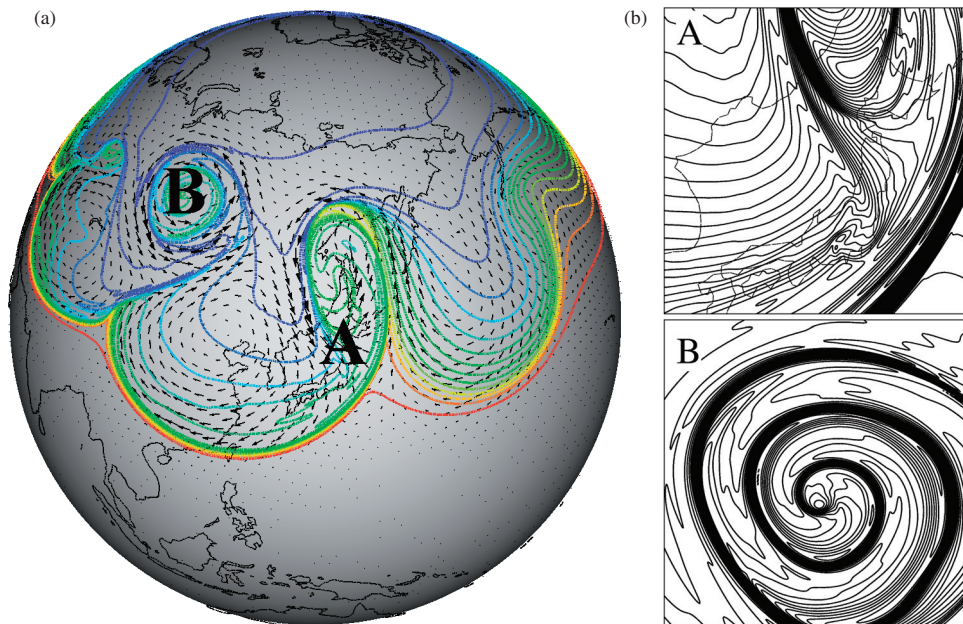


Fig. 5 (a) The surface temperature distribution of the life cycle experiment of baroclinic waves at day 8 using NICAM, glevel-10 (2.5 K interval). (b) Same but zoomed up in region A and B (0.5 K interval).

results implies that the nonhydrostatic effect is not important for the statistical structure at this resolution.

The second test case is the life cycle experiment of baroclinic waves, which is proposed by Polvani and Scott (2002) as a standard experiment of the dynamical core. This test case compares deterministic stage of the nonlinear evolution of extra-tropical cyclones for about 10 days. We have succeeded in the simulation at the resolution of glevel-10 ($\Delta x \approx 7.5\text{km}$) using 80 processor nodes (PNs) of the ES. Different from the original set-up, we use smaller value of the diffusion coefficient $\nu = 7.6 \times 10^{11} \text{ m}^4 \text{ s}^{-1}$, which corresponds to the decay time of 1.15h for the smallest length scale $\Delta x = 7.5\text{km}$. Figure 5(a) shows the temperature distribution just above the surface at day 8. As seen in Fig.5(b), the sharp temperature gradient at the fronts (region A) and the rolling up of vorticity near the center of the occluded cyclone (region B) are well captured.

4. Computational performance of NICAM

From the beginning of this project, NICAM has been designed to run efficiently on massively parallel vector-based supercomputer. In order to gain much higher parallel efficiency, we further optimize NICAM on the ES by mainly

improving the communication procedure; communication frequency in one time step is reduced, overlap of other processes with communication process is considered, the effective vectorized-loop (vertical or horizontal) is chosen, and unnecessary barrier synchronizations is avoided. After these improvement, the communication time is halved in comparison to that of the original code on the condition of glevel-8 / 100 layers using 20 PNs of the ES. Although the vector operation ratio in subroutines mainly used had already been over 98 % even in the original code, we further improved several subroutines by avoiding multiple calculations and reducing the data access to the memory.

We compared the computational performance between the optimized NICAM and AFES by performing the HSTC with 32 vertical layers and 80 PNs being fixed. Figure 6 and Table 1 give the summary of comparison results. The line with black rectangles in Fig.6(a) indicates the elapse times of one time step of NICAM. If we consider that two-grid scale structures are resolvable in NICAM, the resolution of glevel-7 roughly corresponds to that of T319 in the spectral transform model because the mean grid interval for glevel-7 grid system is about 60 km and the truncation wavelength for T319 is about 120km. The line for NICAM in Fig.6(a) is close to N^2

Table 1 The available time intervals and elapse times for 1-day simulation.

(a) AFES						
resolution	T159	T319	T639	T1279	T2559	
Δt_{max} [s]	400	200	100	50	25	
1 day simulation time[s]	8.02	27.9	184	1880	24900	
(b) NICAMhline						
resolution	glevel-7	glevel-8	glevel-9	glevel-10	glevel-11	
Δt_{max} [s]	450	225	113	57	29	
1 day simulation time[s]	6.70	32.1	210	1520	12200	

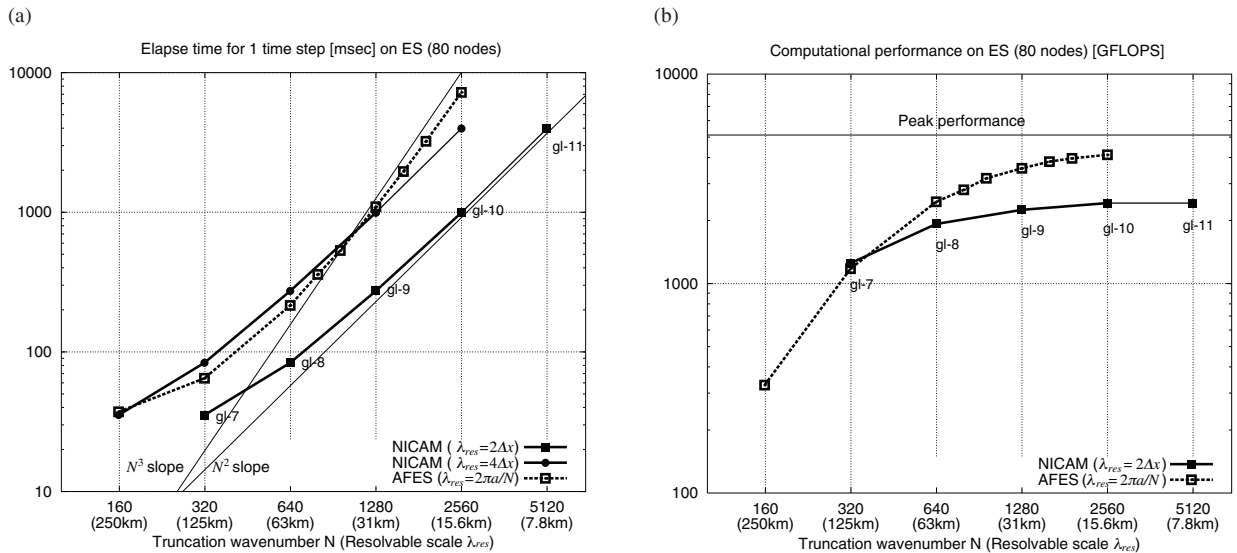


Fig. 6 Comparison of computational performance between NICAM and AFES. λ_{res} stands for the resolvable scale on the equator.

slope in higher resolutions. The reason of this tendency is that the flops value is almost saturated at glevel-10 as shown in Fig.6(b). The performance at glevel-11 is estimated as an extrapolation from that at glevel-9 and 10. Assuming that the flops value of glevel-11 is the same as glevel-10, the slope of the elapse time of one time step from glevel-10 to 11 should be on the N^2 line. On the other hand, the line of AFES in Fig.6(a) (the line with white rectangles) is close to N^3 slope in higher resolutions than T1279. This is partly because the calculation amount of Legendre transformation becomes dominant over the other processes and partly because the flops value becomes saturated as shown in Fig.6(b).

The available time interval without numerical instabilities is also an important factor. By performing 1000 days integration on the condition of HSTC, we investigated the maximum time intervals Δt_{max} as 50 sec increment of Δt for T159 (AFES) and for glevel-7 (NICAM), respectively. Table 1(a) and (b) show the results of Δt_{max} at these resolutions (bold letters). We can presume the maximum time intervals in higher resolutions than glevel-7 for NICAM, because this model employ a quasi-uniform grid; if the resolution becomes double, the maximum interval becomes half. For AFES, the criterion for the maximum time interval is not clear but it is empirically known that the maximum time interval is inversely proportional to the truncation wavenumber. These estimated values are shown in Table 1. Using the maximum time interval and the elapse time of one time step, the elapse times required for 1-day simulation can be estimated for each of models (the third line of each table).

In general, the computational performance depends on the computer architecture, the degree of code optimization, and so on. However, since both AFES and NICAM are aimed to be performed on the ES and are well tuned for vectorization and parallelization, it is appropriate to compare the computational performances on the ES. One point at issue is the physical meanings of the shortest wave of the gridpoint model. If two-grid-scale structures are considered to be resolvable in the gridpoint model, the corresponding resolutions are glevel-7 and T319, or glevel-8 and T639, and so on. Actually, we confirmed that the results of the HSTC are almost the same between NICAM at glevel-7 and AFES at T319. On the other hand, one regards a two-grid-scale wave as a computational noise in the gridpoint model and argues that scales that have physical meanings are limited to the four-grid-scale in the gridpoint model. In this case, the line with black rectangles in Fig.6(a) is shifted to the left line with black circles; the corresponding resolutions become glevel-7 and T159, or glevel-8 and T319, and so on. Even if we employ the latter interpretation of the resolution, Table 1 shows a fact that at this optimization stage NICAM has computational advantage over AFES in the higher resolution than about T1000.

5. Summary and further tasks

We are continuing the development of the global nonhydrostatic model called NICAM at Frontier Research System for Global Change. The model development is going on with parallel paths including a regional nonhydrostatic model, which is based on the same conservative nonhydrostatic scheme as used in NICAM. This regional model is mainly used for investigation of physical processes; it is believed that one of the ambiguities of the current model results comes from lack of the realistic radiation-cloud interactions, so that this regional model will be used for investigation of this processes and also for validation and improvement of cumulus parameterization.

In this paper, we showed the results of several validation test cases for our regional model and global one. The obtained results encourage our new model development. The computational efficiency of our global model NICAM on the ES is also examined. It indicates that NICAM is superior to AFES, which is a well-tuned spectral transform model on the ES, in the higher resolution than about T1000.

Now, only the dynamical core of NICAM has just been completed. There are many things to do to complete NICAM as a climate model. Appropriate physical processes must be installed. Although the ultimate goal is to run climate simulations with explicitly resolving cumulus convection, we suppose that it will be difficult to occupy the ES by running NICAM at the resolution of glevel-10, i.e., about 7.5km grid interval, for several tens of years simulation. The practical approach is to use a coarser resolution grid system of glevel-8 or 9 (10-30km) for such a long time simulation. We need to consider appropriate physical processes for this resolution, particularly for representation of cumulus convection. Besides the physical processes, we need to consider other various problems on the dynamical core itself; the advection scheme on the icosahedral grid, improvement of topography treatment, and so on.

Acknowledgment

The authors would like to thank the AFES Working Group of the Earth Simulator Center for kindly providing us the AFES code. All the simulations of NICAM shown in this study were done using the Earth Simulator.

References

- Gross, E. S., Bonaventura, L., Rosatti, G., 2002. "Consistency with continuity in conservative advection schemes for free-surface models." *Int. J. Numer. Meth. Fluids*, **38**, pp.307-327.
- Held, I. M., Suarez, M. J., 1994. "A proposal for the inter-comparison of the dynamical cores of atmospheric general circulation models." *Bull. Am. Meteorol. Soc.*, **73**, pp.1825-1830.

- Nasuno, T., Saito, K., 2002. "Resolution dependence of a tropical squall line." *submitted to Mon. Wea. Rev.*
- Numaguti, A., Takahashi, M., Nakajima, T., Sumi, A., 1995. "Development of an atmospheric general circulation model. Climate system dynamics and modeling." *Tech. Rep. of CCSR.*, pp.1-27.
- Ohfuchi, W., Enomoto, T., Takaya, K., Yoshioka, M., 2003. "10-km mesh global atmospheric simulations." *Proceeding of 10th ECMWF Workshop on the Use of High Performance Computing, Realizing Teracomputing.* in press.
- Ooyama, K.V., 2001. "A dynamic and thermodynamic foundation for modeling the moist atmosphere with parameterized microphysics." *J. Atmos. Sci.*, **58**, pp.2073-2102.
- Polvani, L., Scott, R., 2002. "An initial-value problem for testing the dynamical core of atmospheric general circulation model." *submitted to Mon. Wea. Rev.*
- Redelsperger, J.-L., Brown, P. R. A., Guichard, F., Hoff, C., Kawashima, M., and K. Nakamura, S. L., Saito, K., Seman, C., Tao, W. K., Donner, L. J., 2000. "A GCSS model intercomparison for a tropical squall line observed during TOGA-COARE I: Cloud-resolving model." *Quart. J. Roy. Meteor. Soc.*, **126**, pp.823-863.
- Satoh, M., 2002a. "Conservative scheme for the compressible non-hydrostatic models with the horizontally explicit and vertically implicit time integration scheme." *Mon. Wea. Rev.*, **130**, pp.1227-1245.
- Satoh, M., 2002b. "A tracer advection scheme consistent with mass conservation in a nonhydrostatic split-explicit model." *Proceeding of 2002 autumn meeting of Meteorological Society of Japan*, A306 (in Japanese).
- Satoh, M., 2003. "Conservative scheme for a compressible non-hydrostatic model with moist processes." *Mon. Wea. Rev.*, **131**, pp.1033-1050
- Shingu, S., Takahara, H., Fuchigami, H., Yamada, M., Tsuda, Y., Ohfuchi, W., Sasaki, Y., Kobayashi, K., Hagiwara, T., Habata, S., Yokokawa, M., Itoh, H., Otsuka, K., 2002. "A 26.58 tflops global atmospheric simulation with the spectral transform method on the earth simulator." *The 2002 ACM/IEEE SC2002 Conference*, Nov.16-22 2002. http://www.sc-2002.org/program_tech.html.
- Tomita, H., Satoh, M., Goto, K., 2002. "An Optimization of the Icosahedral Grid Modified by Spring Dynamics." *J. Comput. Phys.*, **183**, pp.307-331.
- Tomita, H., Satoh, M., Goto, K., 2003. "Global Nonhydrostatic Dynamical Core on the Icosahedral Grid part I: Model description and fundamental tests." *preparation for submitting.*
- Tomita, H., Tsugawa, M., Satoh, M., Goto, K., 2001. "Shallow Water Model on a Modified Icosahedral Geodesic Grid by Using Spring Dynamics" *J. Comput. Phys.*, **174**, pp.579-613.
- Xiao, F., Okazaki, T., Satoh, M., 2003. "An accurate semi-Lagrangian scheme for rain drop" *Mon. Wea. Rev.*, in press.

正二十面体格子を用いた全球非静力高解像度大気大循環モデルの開発

利用責任者

佐藤 正樹 地球フロンティア研究システム モデル統合化研究領域 サブリーダー

著者

佐藤 正樹 地球フロンティア研究システム モデル統合化研究領域 サブリーダー

富田 浩文 地球フロンティア研究システム モデル統合化研究領域 研究員

後藤 浩二 NEC第一コンピュータ事業本部 HPC販売促進本部 サイエンス技術部

那須野智江 地球フロンティア研究システム モデル統合化研究領域 研究員

現在、地球フロンティア研究システムでは、新しい大気大循環モデルの開発が行われている。このモデルは、正二十面体格子を用いた非静力学モデルで、NICAMと呼ばれている。目標とする解像度は、水平格子間隔10km以下、鉛直格子間隔100mである。現段階で、NICAMの力学過程がほぼ完成し、様々なテスト実験(簡単な設定の強制を入れた気候実験、理想的な初期条件を用いた低気圧のライフサイクル実験等々)を行っているところである。地球シミュレータ上で、このモデルの最適化を行い、短い期間の設定であるが、全球7.5km格子間隔の数値実験が可能であることを示した。同時に、AFES(AGCM For Earth Simulator)を用いて、既存のスペクトル法とNICAMとの計算パフォーマンスを比較した。10km格子間隔以下では、NICAMの方が効率良く計算できることが分かった。一方、NICAMの開発と並行して、NICAMのサブセットモデルとしての領域非静力学モデルも開発中である。この領域モデルは、NICAMと同じ力学スキームを用いており、既にいくつかの物理過程の実装が行われている。主に、雲放射相互作用等のプロセス研究に使われる。同時に、NICAMで用いられる物理過程のテストフレームになっている。この意味で、NICAMと同様に本プロジェクトの成功の可否を握る重要なモデルである。

キーワード：正二十面体格子、全球非静力学モデル